Title

Generate a new crucian carp (*Carassius auratus*) strain without intermuscular bones by knocking out *bmp6*

Youy Kuang[1,2,3,4,*], Xianhu Zheng[1,2,3], Dingchen Cao[1,2,3], Zhipeng Sun[1,2,3], Guangxiang Tong[1,2,3], Huan Xu[1,2,3], Ting Yan[1,2,3], Shizhan Tang[1,2,3], Zhongxiang Chen[1,2,3], Tingting Zhang[1,2,3], Tan Zhang[1,2,3], Le Dong[1,2,3], Xiaoxing Yang[1,2,3], Huijie Zhou[1,2,3], Weilun Guo[1,2,3], Xiaowen Sun[1,2,3,*]

Affiliation

1. National and Local Joint Engineering Laboratory for Freshwater Fish Breeding, No. 232, Hesong Street, Daoli District, Harbin 150070, China
2. Key Laboratory of Freshwater Aquatic Biotechnology and Breeding, Ministry of Agriculture and Rural Affairs, No. 232, Hesong Street, Daoli District, Harbin 150070, China
3. Heilongjiang River Fisheries Research Institute of Chinese Academy of Fishery Sciences, No. 232, Hesong Street, Daoli District, Harbin 150070, China
4. Heilongjiang Provincial Key Laboratory of Hard Tissue Development and Regeneration, The Second Affiliated Hospital of Harbin Medical University, Harbin 150081, China

E-Mail:

Youyi Kuang: kuangyouyi@hrfri.ac.cn
Xianhu Zheng: zhengxianhu@hrfri.ac.cn
Dingchen Cao: caodingchen@hrfri.ac.cn
Zhipeng Sun: sunzhipeng@hrfri.ac.cn
Guangxiang Tong: tongguangxiang@hrfri.ac.cn
Huan Xu: xuhuan@hrfri.ac.cn
Ting Yan: yanting@hrfri.ac.cn
Shizhan Tang: tsz2007@163.com
Zhongxiang Chen: chenzx@hrfri.ac.cn
Tingting Zhang: 1260242608@qq.com
Tan Zhang: tan_zhg@sina.com
Le Dong: 610478772@qq.com
Xiaoxing Yang: 1393072122@qq.com
Huijie Zhou: 1668312678@qq.com
Weilun Guo: 1172141357@qq.com
Xiaowen Sun: sunxw2002@163.com

* To whom correspondence should be addressed.
Youyi kuang, E-Mail: kuangyouyi@hrfri.ac.cn; Tel: +86-451-87930951; Xiaowen Sun, E-Mail: sunxw2002@163.com；Tel:+86-451-84842646

Abstract

Elimination of intermuscular bones (IMBs) is vital to the aquaculture industry of cyprinids. In our previous study, we characterized *bmp6* as essential in the development of IMBs in zebrafish. Knockout of *bmp6* results in the absence of IMBs in zebrafish without affecting growth and reproduction. Therefore, we hypothesized that *bmp6* could be used to generate new cyprinid strains without IMBs by gene editing. In this study, we established a gene editing strategy for knocking out the two orthologs of *bmp6* in diploid crucian carp (*Carassius auratus*). We obtained an F_3 population with both orthologs knocked out, in which no IMBs were detected by bone staining and X-ray, indicating that the new strain without IMBs (named WUCI strain) was successfully generated. Furthermore, we extensively evaluated the performance of the new strain in growth, reproduction, nutrient components, muscle texture and structure, and metabolites in muscle. The results showed that the WUCI strain grew faster than the wild-type crucian carp at 4-month-age. The reproductive performance and flesh quality did not show significant differences between the WUCI strain and wild-type crucian carp. Moreover, the metabolomics analysis suggested that the muscle tissues of the WUCI strain significantly enriched some metabolites belonging to the Thiamine metabolism, Nicotinate and Nicotinamide Metabolism pathway, which plays beneficial effects in anti-aging, antioxidant, and anti-radiation damage. In conclusion, we established a strategy to eliminate IMBs in crucian carp and obtain a WUCI strain whose performance was expected compared to the wild-type crucian carp; meanwhile, the WUCI strain enriched some beneficial metabolites to human health in muscle tissue. This study is the first report that a cyprinid strain without IMBs, which could be stably inherited, was obtained worldwide; it provided excellent germplasm for the cyprinids aquaculture industry and a useful molecular tool for eliminating IMBs in other cyprinids.

Keywords: crucian carp, *Carassius auratus,* a new strain without intermuscular bones, *bmp6*, gene editing, performance evaluation, metabolomics

1. Introduction

Cyprinids are the most important aquaculture species in China, with an annual production of about 27 million tons, occupying around 76% of total freshwater fish aquaculture production. However, the intermuscular bones (hereafter IMBs) severely cause food inconvenience and may even lead to physical injuries such as being stuck in the throat. The processing of fish products (such as fish balls) is also hindered. The genetic breeding of IMBs of cyprinids has become an increasing interest in China[1–3].

The genetic breeding of IMBs in cyprinids began in the 1960s[4], but there has been no progress until the last decade. With the development of biotechnology, some progress has been made in the genetic breeding of IMBs. For example, Xu et al.[5] found a mutant with normal growth and absence of IMBs from a gynogenesis population of grass carp(*Ctenopharyngodon idellus*); Peruse et al. [6] obtained a population with IMBs deficient in *Colossoma macropomum* by X-ray scan; Wu et al.[7] obtained a population with a 5.7% reduction in the count of IMBs by crossing *Megalobrama amblycephala* and *Culter alburnus*, indicating that varieties with less count of IMBs can be obtained by crossbreeding. Lin et al.[8] reported that hybrid crucian carp (*Carassius auratus*) had a smaller number of IMBs than wild crucian carp, and the count of IMBs of crucian carp could be reduced by polyploid breeding and crossbreeding methods; Cao et al. [9] concluded that mirror carp (*Cyprinus carpio*) could be an excellent candidate for genetic selection to reduce IMBs. In terms of genetic and molecular breeding, Xiong et al.[10] found that the heritability of the number of IMBs differed in different parts of blunt snout bream (*Megalobrama amblycephala*); Wan et al. [11] identified single nucleotide polymorphism (SNP) markers associated with the count of IMBs in *Megalobrama amblycephala*. The counts of IMBs were significantly different among common carp (*Cyprinus carpio*) species/strains and families[9,12]. However, the heritability of IMBs was low, with a value of 0.15[12]. Eight significant QTL intervals were obtained in the QTL analysis of the number of IMBs in mirror carp, which explained 7.7-25.9% of the phenotypic variation[12].

From the above statements, it is clear that genetic improvement of IMBs can be carried out by artificial selection, cross breeding, gynogenesis, polyploid breeding, and molecular marker-assisted selection; however, there is still no breakthrough in reducing more than 50% of IMBs. With the development of gene editing technology, the genes and regulatory elements affecting the development of IMBs have been characterized. For example, Nie et al.[13] knocked out *scxa* in zebrafish and obtained a mutant with more than 70% reduction in the count of IMBs, rib hypoplasia, and defective septal development [13,14] . In our previous study, we characterized that *bmp6* regulates the development of IMBs in zebrafish[15], and its knockout causes the complete absence of IMBs in zebrafish without affecting the growth, muscle, and bone development of zebrafish[15–18]. Therefore, we hypothesize that *bmp6* could be used to generate new cyprinid strains without IMBs by gene editing.

In this study, we generated a new crucian carp (*Carassius auratus*) strain without IMBs (hereafter WUCI strain) by knocking out *bmp6* and demonstrated that knockdown of *bmp6* did not affect the growth, and nutritional quality of the strain; we also conducted a metabolomics analysis of muscle to explore the effects of *bmp6* on substance synthesis and metabolism. This study provided an excellent germplasm for the cyprinids aquaculture industry and a useful molecular tool for eliminating IMBs in other cyprinids.

2. Materials and methods

2.1 Ethics statement

In this study, all animal procedures were conducted according to the guidelines for the care and use of laboratory animals of Heilongjiang River Fisheries Research Institute (HRFRI), Chinese Academy of Fishery Sciences (CAFS). The studies in animals were reviewed and approved by the Committee for the Welfare and Ethics of Laboratory Animals of HRFRI, CAFS. The gene editing studies were approved by the Committee for Genetic Modification Organism (GMO) Safety Management (Approved ID: HRFRI-GMO-201801).

2.2 Experimental fish

The diploid crucian carp (*Carassius auratus*, 2n=100) used in this study were cultured in the Hulan Experimental Station of HRFRI. Parental fish were reared in a 700m^2 pond and injected with oxytocin drugs, including luteinizing hormone-releasing hormone (LRH-2, 4ug/kg body weight); domperidone (DOM, 1mg/kg body weight), and human chorionic gonadotropin (HCG, 100 U/kg body weight) for spawning. The fertilized eggs were incubated in 24cm×20cm×24cm incubation tanks at 22℃ ～ 23℃. After hatching, larvae were fed 4 times/day of Artemia until they grew up to 2cm-3cm in body length; the larvae were moved to a 500m^2 pond and fed artificial feed 2 times/day.

2.3 *Bmp6* knockout

Because the crucian carp underwent the fourth round of genome duplication event[19], there are two orthologs of *bmp6* in the crucian carp genome. To identify the two orthologs, the cDNA and protein sequence of zebrafish *bmp6* were aligned to the crucian carp genome [19] using Blast tools, and the two orthologs were validated by the annotation of Ensembl(http://www.ensembl.org), which were ENSCARG00000018439(*bmp6a*) and ENSCARG00000056616(*bmp6b*).

The *bmp6a* and *bmp6b* knockout was carried out according to the method described by Xu et al.[15] and described as follows. The target sites for CRISPR/Cas9 knockout were designed using the CHOPCHOP service[20] (Supplementary Table S1). The sgRNA was synthesized using the NEB HiScribe T7 Fast and Efficient RNA Synthesis Kit (NEB E2050S, MA, USA). After mixing 5μM~10μM sgRNAs of *bmp6a* and *bmp6b* and 5μM Cas9 protein (M0646, NEB, MA, USA), 1nL mixture was micro-injected into single-cell embryos. The embryos were incubated at 22~23℃ as described above.

2.4 Mutants screening

After four months of culture, fish were labeled with PIT tags, and fin clips were collected for DNA extraction. The fin clips were lysed with 100μl solution consisting of 0.5 mg/ml proteinase K, 10 mmol/L pH 8.0 1 M Tris, 50 mmol/L KCl, 0.3% Tween 20, 0.3% NP 40 at 55°C for 6 h and 98°C for 10 min. After lysis, the lysate was mixed and centrifuged at 1000-2000 rpm for 2 min, and the supernatant was taken for PCR amplification.

The method for screening mutants is illustrated in Fig. 2(c). In this procedure, PCR amplification was performed using the method described by Tong et al. [21]and was briefly described as follows. Two pairs of primers were used for PCR amplification, one of which was the target primer for amplifying the target fragment

(Supplementary Table S2), and the other was the index primer for indexing samples. A 2-step amplification was performed: firstly, the PCR was carried out using 10 μL volume, including genomic DNA supernatant 1 μL, 1 μmol/L forward and reverse target primers 0.5μL, 2× Dream Taq Master Mix (Thermo Fisher, CA, USA) 5μL, the PCR was performed with 95°C for 3 min, followed by 10cycles of 95°C 30 s, 60°C 30 s, 72°C 30 s; 72°C for 2 min; the second PCR amplification was performed by adding 0.5μL of 5μmol/L forward and reverse index primers to the first step PCR product, and the PCR program was set to 95°C for 2 min; 6 cycles of 95°C 30 s, 58°C 30 s, 72°C 30 s; and 15 cycles of 95°C 30 s, 72°C 30s, finally 72°C 2min.

After PCR amplification, PCR products were mixed in equal amounts, DNA sequencing libraries were constructed using the TrueSeq library prepare kit, and 300bp Pair-End sequencing was performed using the Illumina MiSeq sequencing platform. The data obtained by MiSeq were first used to identify the loci and samples with the method described by Tong et al. [21] , followed by analysis with CRISPResso2 [22] to screen the mutants and calculate the somatic mutation rate of each sample.

2.5 Intermuscular bone observation

We used skeleton staining, X-ray, and micro-CT to observe IMBs. Skeleton was stained using Alizarin red with the method described by Yang et al. [18]and observed using the Zeiss Stereo Discovery V8 system (Carl Zeiss, Jena, Germany), the X-ray observation was performed using Faxitron MX-20 X-ray System(Faxitron, MA, USA), and the Quantum GX micro-CT Imaging System (PerkinElmer, MA, USA) with 70 KV, 88μA, and 14 min scan time was used for micro-CT. Around 50dph~60dph fish were used for bone staining, and four-month-old fish was used for X-ray and micro-CT scan.

2.6 Growth and reproductive performance evaluation

After one month of culture in a pond, 600 fingerlings of WUCI strain with BW of 4.6±0.42g and 600 fingerlings of wild-type crucian carp with BW of 4.2±0.55g were raised in a 500m^2 pond. During the culture, the SL and BW were measured each month. At the age of 4 months, 50 individuals of WUCI strain and wild-type crucian carp were randomly chosen to measure the BW and SL. Furthermore, the gonad of 30 individuals from each group was dissected for weighting and histological examination according to Gan et al. [23] . The absolute fecundity and relative fecundity were calculated with the method described by Franěk et al.[24].

2.7 Flesh quality evaluation

Thirty 4-month-old fish from each group were selected to evaluate flesh quality. For the texture analysis, the dorsal muscle with size of 1cm^3 and 2cm*1cm*1cm was dissected to measure the hardness, cohesiveness, springiness, gumminess, chewiness, and shear force using a TMS-Pro texture meter (Food Technology Corporation, VA, USA). The remained muscle tissues were dissected to measure the nutrient components, and muscles from 10 individuals were pooled; 3 pooled samples of each group were tested. Moreover, the content of trace elements was measured using dorsal muscle and liver tissues from 5 fish of each group. Additionally, dorsal muscles from 5 fish of each group were dissected for histological analysis according to Yang et al.[16].

The nutrient components, including proximate compositions (moisture, crude ash, crude protein, and crude lipid), amino acid compositions, fatty acid compositions, and

vitamin compositions (A, B1, B2, D, and E) were measured in Qingdao Sci-tech Innovation Quality Testing Co., Ltd. according to the national standards of China. The contents of trace elements, including Mg, Mn, Fe, Zn, Cu, Se, and K, were measured using inductively coupled plasma-mass spectrometry (ICP-MS, Agilent 7500cx, USA).

2.8 RT-qPCR of *bmp6a* and *bmp6b*

Ten organs, including intestine, liver, dorsal muscle, caudal muscle, brain, spleen, skin, gill, kidney, and heart from 6 wild-type crucian carp at 4-month-age were dissected for total RNA extraction using Trizol (Thermo Fisher, CA, USA). RNA quality was measured using Nanodrop 8000 (Thermo Fisher, CA, USA), and the quantity of RNA was measured using the Qubit3 kit (Thermo Fisher, CA, USA). The RNA was reverse-transcribed with the Revert Aid^{TM} First-Strand cDNA Synthesis Kit (Thermo Fisher, CA, USA). The qPCR was analyzed with primers listed in Supplementary Table S3, and *β-actin* was used as the reference gene. The RT-qPCR was carried out using 10 μL volume, including 1 μL of 50ng/μL cDNA, 0.5μL of 10μM forward and reverse primer, 5μL of 2× Luna Universal qPCR Master Mix (NEB, MA, USA). The amplification program was set as follows: 95 ℃ for 15s, followed by 40 cycles of 95℃ 15s and 60℃ for 30s. The qPCR was performed using the QuantiStudio 6 Flex Real-Time PCR System (Thermo Fisher, CA, USA).

2.9 RNA fluorescence in situ hybridization

We used the caudal muscle tissues of 60dph wild-type crucian carp to detect the spatial expression of bmp6a and bmp6b. The RNA fluorescence in situ hybridization was carried out with the SABER-FISH protocol according to Kishi et al.[25,26]. The probes were designed by the method proposed by Beliveau et al. [27] and listed in Supplementary Table S4. the mRNA of bmp6a and bmp6b was detected using Alexa Fluor 532 probes, and the nucleus was stained using DAPI dye (Thermo Fisher, CA, USA). The cryosections were observed using a fluorescence microscope (OLYMPUS BX53, Japan), and the images were processed by ImageJ.

2.10 Metabolomics analysis

The dorsal muscle tissues of 15 fish from each group were dissected and frozen in liquid nitrogen for metabolomics analysis. The tissues were grounded with liquid nitrogen, and after resuspending with prechilled 80% methanol by vortex, the samples were incubated on ice for 5min and were centrifuged for 20min at 15000g and 4°C; the supernatants were diluted to a final concentration of 53% methanol by LC-MS grade water and transferred to fresh Eppendorf tubes. After centrifugation at 15000g and 4°C for 20min, the supernatant was subjected to the LC-MS/MS system. The UHPLC-MS/MS analyses were carried out using a Vanquish UHPLC system (Thermo Fisher, Germany) coupled with an Orbitrap Q Exactive HF-X mass spectrometer (Thermo Fisher, Germany) in Novogene Co., Ltd. (Bejing, China).

The original file obtained by UHPLC-MS/MS was imported into Compound Discoverer 3.1 (CD3.1) software for spectrogram processing with parameters of retention time tolerance of 0.2 min, an actual mass tolerance of 5ppm, signal intensity tolerance of 30%, and signal/noise ration of 3. After normalization to the total spectral intensity, the normalized peak intensities were used to predict the molecular formula based on additive ions, molecular ion peaks, and fragment ions. The databases of mzCloud(https://www.mzcloud.org), mzVault, and MassList database were used to

match the peak and obtain accurate qualitative and relative quantitative results.

The quantitative matrix of metabolites was analyzed by multivariate statistical analysis, including principal component analysis (PCA) and partial least squares discriminant analysis (PLS-DA) to reveal the differences in metabolic patterns among different groups. The univariate analysis (Student's t-test) was used to calculate the statistical significance, the metabolites with P-values<0.05, variable importance in the projection (VIP) value >1.0, and fold-change(FC) of WUCI vs. wild-type ≥1.5 or ≤0.667 were considered to differential metabolites. After annotating with KEGG, HMDB (https://hmdb.ca/metabolites), and LIPIDMaps database (http://www.lipidmaps.org), pathway analysis was carried out using MetaboAnalyst 5.0[28]

3. Results

3.1 Expression pattern of duplicated *bmp6* in crucian carp

Bmp6 has been indicated to co-express in the myoseptum with osteoblast marker gene *sp7*, tendon progenitor marker gene *scxa,* and tenocyte marker gene *tnmd* and *xirp2a* [15] . However, *bmp6* had two orthologs (*bmp6a*: ENSCARG00000018439; *bmp6b*: ENSCARG00000056616) in the crucian carp genome caused by the fourth whole-genome duplication event (Fig. 1(a)) [19] . To explore whether the two duplicated copies had a similar function to the development of IMBs in crucian carp, we investigated the expression levels in 9 tissues using RT-qPCR; *bmp6a* had a high expression level in dorsal muscle, caudal muscle, and skin; *bmp6b* had a high expression level in liver and gill (Figs. 1(b), (c)); Supplementary Figs. S1, S2). The spatial expression of *bmp6a* and *bmp6b* in caudal muscle detected by RNA fluorescence in situ hybridization (RNA-FISH) showed that both orthologs were expressed in the myoseptum(Figs. 1(d), (e)); Supplementary Fig. S3). These results indicated that both orthologs might function in IMB's development despite the expressed levels.

3.2 Pipeline for *bmp6* gene editing in crucian carp

According to the expression in muscle, *bmp6a* and *bmp6b* should be knocked out simultaneously to obtain individuals without IMBs. In order to rapidly establish the WUCI strain, we designed a two-round gene knockout and mating strategy in this study (Fig. 2(a)). In this strategy, three target sites were designed in exon 1 of *bmp6a* and *bmp6b*, respectively (Fig. 2(b)). Firstly, sgRNAs of *bmp6a* and *bmp6b* were used for the first round of multiplex gene knockout to construct the F_0 generation, and the mutants of F_0 generation were screened by high-throughput sequencing using PCR products of target sites (Fig. 2(c)). The mutants with somatic mutation rates more than 95% (*bmp6a* or *bmp6b*) were selected for natural mating, and the second round of multiplex gene knockout of *bmp6a* and *bmp6b* was performed in their fertilized eggs to construct the F_1 generation. In the F_1 generation, individuals with somatic mutation rates of more than 95% *bmp6a* and *bmp6b* were scanned by X-ray to screen individuals without IMBs, which were used to construct the F_2 generation population by natural mating. Genotypes and counts of IMBs of the F_2 generation were screened, and individuals without IMBs were used for natural mating to reproduce the F_3

generation. Individuals of the F_3 generation were used for evaluating the growth and fecundity performance, nutrient components, and metabolomics analysis.

3.3 Generation of a new strain without intermuscular bones

Using this pipeline, we carried out *bmp6* gene editing in crucian carp. Among 668 F0 progenies, 511 mutants were screened, including 117 mutants with *bmp6a* and *bmp6b* mutated in somatic cells (Fig. 2(d), Supplementary Table S5). The somatic mutation rate of *bmp6a* and *bmp6b* in F_0 mutants were 52.20%~96.10% and 20.80~99.80, respectively (Fig. 2(d), Supplementary Table S6), with the mean value of 72.1% and 75.74%, respectively. The percent of mutants with somatic mutation ratio ⩾95% of *bmp6a* and *bmp6b* was 0.61% and 27.1%, respectively.

After the knockout of *bmp6a* and *bmp6b* for the second time using F_0 adults, 1130 F_1 progenies were obtained, among which 947 mutants were screened, including 630 mutants with *bmp6a* and *bmp6b* mutated in somatic cells (Fig. 2(d). Supplementary Table S5). The somatic mutation rate of *bmp6a* and *bmp6b* in F_1 mutants were 61.70%~100% and 36.70%~100%, respectively (Fig. 2(d), Supplementary Table S6), with the mean value of 93.4% and 97.25%, respectively. The percent of mutants with somatic mutation ratio ⩾95% of *bmp6a* and *bmp6b* was 64.65% and 89.58%, respectively.

A comparative analysis showed that the somatic mutation rates of *bmp6a* or *bmp6b* in the F_1 mutants were significantly higher than those in the F_0 mutants ($P<0.0001$, Fig. 2(d), Supplementary Table S5). The number of mutants with both genes mutated and the number of mutants with a somatic mutation rate more than 95% in the F_1 generation was also significantly higher than those in the F_0 generation ($P<0.0001$, Fig. 2(e), Supplementary Table S6), and the somatic mutation rate of samples with both genes mutated in F_1 mutants was also significantly higher than in F_0 mutants ($P<0.0001$, Fig. 2(e), Supplementary Table S6). These results indicated that the two-round gene knockout strategy significantly increased the mutation rate and the number of samples with high mutation rates of both genes, resulting in the rapid establishment of homozygous mutated lines.

In the F_1 generation, 270 progenies with 95% somatic mutation rate of *bmp6a* and *bmp6b* were screened, among which 35 mutants without IMBs were obtained using X-ray scanning (Fig. 3(a), Supplementary Figs. S4-S7), accounting for 12.96%; additionally, 110 mutants with more than 50% reduction of the count of IMBs were screened, accounting for 40.74%. The F_2 population was constructed by natural mating with the 35 F_1 mutants without IMBs; among 1500 F_2 progenies, 285 individuals without IMBs were obtained, accounting for 19.00%, and 380 individuals with the count of IMBs reduced by more than 50%, accounting for 25.33% (Fig. 3(b)). Furthermore, individuals without IMBs of the F_2 generation were used to construct the F_3 generation population by natural mating, and 41 individuals at 60dph (days post-hatched) were randomly chosen for bone staining, no IMB was found in staining (Fig. 3(c)). We also examined the IMBs by X-ray using 30 individuals at 4 months of age and approved the results (Fig. 3(d)). These results indicated that the WUCI strain was generated successfully.

3.4 Growth of the new strain

For evaluating the growth performance of the WUCI strain, 600 one-month-old fingerlings of WUCI strain with body weight (BW) around 4.6±0.42g and body length(SL) around 4.94±0.38mm and 600 one-month-old fingerlings of wild-type crucian carp with BW around 4.2±0.55g and SL approximately 4.79±0.35mm were

cultured for three months at a 500m^2 pond, the BW and SL were measured each month. The relationship between BW and SL of the WUCI strain was similar to that of the wild-type crucian carp (Supplementary Fig. S8). The comparisons showed that the SL and increment of SL per month of the WUCI strain were significantly higher than that of wild-type crucian carp at 2, 3, and 4 months of age(Figs. 4(a), (b), Supplementary Table S7); there was no significant difference in specific growth rate(SGR) of SL per month between the WUCI strain and wild-type crucian carp at 2,3months of age, whereas, a significant difference(P<0.001) in SGR of SL at four months of age was observed(Fig. 4(c), Supplementary Table S7). The growth of BW was similar to that of SL (Figs. 4(d)-(f), Supplementary Table S7). Based on the above analysis results, it can be concluded that the WUCI strain at 2~4-month-old grew faster than the wild-type crucian carp.

3.5 Nutrient components of the new strain

The nutrient components in muscle tissue of 4-month-old WUCI strain and wild-type crucian carp were determined. We analyzed the proximate composition, total saccharide, vitamins, fatty acids, and amino acids (Supplementary Table S8-11). Seventeen kinds of amino acids and 17 types of fatty acids were determined. Among the five vitamins (A, B1, B2, D, and E) we measured, vitamins A and D were not detected. The comparison results showed that there was no significant difference in the contents of nutrient components mentioned above, as well as essential amino acid (EAA), umami amino acid (UAA), essential fatty acid (EFA), polyunsaturated fatty acid (PUFA), Omega3, and Omega6 (Fig. 5, Supplementary Table S8-11). We also measured seven elements in the muscle and liver tissues, including Mg, Mn, Fe, Cu, Zn, Se, and K. The significance test showed that the contents of Fe and Se in the liver of the WUCI strain were significantly higher than those of the wild-type crucian carp. In contrast, the contents of all elements in the muscle did not show a significant difference (Fig. 6, Supplementary Table S12).

3.6 Muscle texture and structure of the new strain

Muscle texture and structure are important to fish flesh quality. The muscle texture analysis showed that the shear force of the WUCI strain was significantly higher than those of wild-type crucian carp(P<0.01) (Fig. 7(a), Supplementary Table S13). In contrast, the hardness of the WUCI strain was significantly weaker than those of wild-type crucian carp(P<0.05) (Fig. 7(b), Supplementary Table S13). Furthermore, the two groups had no significant difference in cohesiveness, springiness, gumminess, and chewiness (Figs. 7(c)-(f), Supplementary Table S13). The PCA analysis result of muscle texture showed that most samples of the WUCI strain were clustered together with those of the wild-type strain and not well distinguished (Supplementary Fig. S9), indicating that no significant difference occurred between the two groups. We also carried out a histological analysis of muscle tissues, and the results showed that the muscle fiber area and density had no significant differences (P>0.05) between the WUCI strain and the wild-type crucian carp (Figs. 7(g)-(j), Supplementary Table S13). These results indicated that the knockout of *bmp6a* and *bmp6b* and the lack of IMBs did not significantly change the muscle texture and structure of the WUCI strain.

3.7 Reproductive performance of the new strain

The comparison analyses showed no significant difference in the weight of ovary and ovarian GSI (Gonadosomatic index, gonad weight/body weight ×100) between the 4-month-old WUCI strain and wild-type crucian carp(P>0.05) (Figs. 8(a),

(b); Supplementary Table S14). The weight of the testis and GSI of the WUCI strain were significantly higher than those of wild-type crucian carp ($P<0.01$ and $P<0.05$, respectively) (Figs. 8(a), (b); Supplementary Table S14). Moreover, no significant difference between the two groups was observed in the absolute female fecundity (total quantity of produced eggs by females) and relative fecundity(the number of eggs per gram of body weight) ($P>0.05$) (Figs. 8(c), (d); Supplementary Table S14). The gonad histological analysis showed that the development of the ovary and testis of the WUCI strain was similar to that of the wild-type crucian carp (Figs. 8(e), (f)). These results suggested that the *bmp6a* and *bmp6b* knockout and the absence of IMBs did not significantly affect the gonad development and the fecundity of the WUCI strain.

3.8 Metabolome analysis

The peaks extracted from all samples and QC were analyzed by PCA, and the results showed that the QC samples in the positive and negative ion modes were clustered together (Figs. 9(a), (b)), indicating that the experiment was robust. The PLS-DA model of two groups was established, and 7-fold cross-validation was performed to characterize the model's stability and reliability (Figs. 9(c), (d)). A total of 863 metabolic ion peaks were extracted, including 546 positive ion peaks and 317 negative ion peaks. Using the parameters of VIP > 1.0, FC > 1.5 or FC < 0.667, and P-value< 0.05, 107 metabolites in the positive ion mode had significant differences, including 28 up-regulated and 79 down-regulated metabolites in the WUCI strain (Supplementary Table S15); in the negative ion mode, 124 metabolites had significant differences, including 5 up-regulated and 119 down-regulated metabolites in the WUCI strain (Supplementary Table S16). These up-regulated metabolites included some metabolites that are beneficial to the organism, such as β-Nicotinamide mononucleotide, DL-Glutamine, Hypoxanthine, Traumatic acid, Thiamine pyrophosphate, and so on (Figs. 9(e)-(l)). KEGG pathway enrichment analysis showed that 46 metabolite pathways were enriched, including Thiamine metabolism, Glutathione Metabolism, Nicotinate and Nicotinamide Metabolism, amino acids metabolism pathways, etc. (Fig. 9(m), Supplementary Table S17, Supplementary Fig. S10).

4. Discussion

The cyprinids aquaculture industry requires varieties with high flesh quality, and the reduction of IMBs is one of the main targets for improving the flesh quality [1,3,29] . Although researchers utilized many approaches to deplete cyprinids IMBs, little progress was obtained until the eruption of the gene editing technology. Based on our previous study [15] , we generated a new crucian carp strain without IMBs by knocking out *bmp6.* This strain has expected performances of growth, reproduction, nutrient value, and muscle texture and structure; significantly, its muscle enriched some beneficial metabolites for human health. According to our knowledge, it is the first report that a cyprinid strain without IMBs, which could be stably inherited, was obtained in the world.

There are two orthologs of *bmp6* in crucian carp; according to the expression in the muscles, it is supposed that the two orthologs should be knocked out simultaneously to obtain mutants with complete depletion of IMBs, which was confirmed by our results (Fig 3b). In general, multiplex gene knockout homozygous strains were obtained by sequential knocking out a single gene or crossing with homozygous lines with a single gene knockout, which is difficult and time-consuming

(around 3~4 generations to get a homozygous line). We established a two-round knockout strategy to obtain homozygous mutants with the simultaneous knockout of *bmp6a* and *bmp6b*. This strategy contains three aspects: firstly, we used three guides to knock out *bmp6a* or *bmp6b*. Wu et al. [30] proved that the simultaneous use of multiple guides could significantly increase the efficiency of functional disruption; we adopted this strategy and obtained mutants in more than 70% of the F_0 generation (Supplementary Table S5, S6). Secondly, the mutants with more than 95% mutation rate of somatic cells were chosen to reproduce the next generation. Generally, the mutation in germ cells was unknown, and we supposed that the gene in germ cells should be mutated if the somatic mutation rate was more than 95%, if we used the fertilized eggs from those F_0 adults to generate the F_1 generation by the second knockout, it could significantly increase the simultaneous mutated probabilities of *bmp6a* and *bmp6b* because the mutation of the F_1 progenies was the accumulation of the mutation inherited from the F_0 germ cells and the mutation caused by the second knockout. This assumption was evidenced by our results, in which the somatic mutation ratio in the F_1 generation was significantly higher than that in the F_0 generation (Figs. 2(d), (e); Supplementary Table S5, S6). Thirdly, the mutants were screened using high-throughput sequencing technology. Genome editing in cultured fishes needs to screen many individuals to obtain as many mutants as possible, which is labor- and time-consumption by traditional methods, such as gel electrophoresis, Sanger sequencing, high-resolution melt curves, etc. Based on our previous study[21], we developed a mutant screening method using high-throughput sequencing of PCR products by amplifying the target fragments using two pairs of primers, one of which was used to amplify the fragment containing the gene editing target sites and the other pair was used to append the index bases of the sample to the PCR product, after sequencing, the data were demultiplexed to individuals and knockout targets which were used to screen the mutants by CRISPResso2 [22] . Using this method, we can obtain the mutants in a time- and cost-efficient way. This strategy has an advantage, i.e., it could reduce the time to establish a new strain with both genes mutated from 3~4 generations to 2 generations; however, the disadvantage is that the strain has multiple alleles (Supplementary Figs. S4-S7).

Using the strategy described above, we obtained the mutants without IMBs in the F_1 population and established the WUCI strain in two generations; the observation of IMB in the F_3 progenies suggested that the trait was stable and inheritable; these results demonstrated that *bmp6* could be used to generate new cyprinids strains without IMBs by gene editing.

Bmp6 is a member of the BMP family, and it regulates many biological processes, such as skeletal development[31], iron metabolism[32], female fertility[33,34], and so on. Although the knockout of *bmp6* had no significant effects on growth and reproductive performance or the development of muscle and skeletal in zebrafish [15–18], it is unknown whether the knockout of *bmp6* affects the performance of the WUCI strain. Here, we comprehensively evaluated growth, reproduction, nutrient quality, muscle structure, and texture between the WUCI strain and the wild-type crucian carp. The results showed that the knockout of *bmp6* did not affect the growth and reproductive performance of the WUCI strain, which was consistent with our previous studies in zebrafish [15–18]. Growth is associated with the development of muscle and skeleton; the skeletal phenotype and the histological section of muscle showed that the musculoskeletal development was normal in the WUCI strain, implying that the function of *bmp6* in the musculoskeletal system might be compensated by others of the BMP family[35]. *Bmp6* is also involved in proliferation,

steroidogenesis, and oocyte development in humans and mammals [33,36–39] functions in a specifies-specific way[40]. Although the mRNA of *bmp6* was detected in oocytes and granulosa cells [41] in zebrafish, there was no enough evidence to show the effect of *bmp6* on female fecundity. The present study and our previous studies showed that the knockout of *bmp6* did not significantly affect the reproductive performance in crucian carp and zebrafish, which implied that *bmp6* might not be the essential gene in the gonadal development of cyprinids, or the function of *bmp6* is compensated by other members of the BMP/TGE-β family; however, more studies are required. The detection of 7 elements in the liver and muscle showed that the content of Fe was higher in the WUCI strain than that in the wild-type crucian carp, which indicated that the iron overload in the liver of the WUCI strain caused by the dysfunction of *bmp6* [32], however, the content of Fe in the muscle of the WUCI strain did not show the significance compared to that of the wild-type crucian carp, which meant the deposited and transferred mechanism of Fe in muscle might be different in the liver.

In addition to evaluating nutrient quality by the traditional method, we performed further analysis of the metabolome. Metabolomics analysis results showed some pathways and metabolites were enriched in the muscle tissue of the WUCI strain, such as Nicotinate and nicotinamide metabolism pathway, Thiamine metabolism pathway, β-Nicotinamide mononucleotide, DL-Glutamine, Hypoxanthine, Traumatic acid, and Betaine. These pathways and metabolites are related to beneficial properties, including anti-aging, anti-oxidative, and anti-radiation damage effects (Fig. 9). Nicotinate and nicotinamide are precursors of the coenzymes nicotinamide adenine dinucleotide (NAD+) and nicotinamide adenine dinucleotide phosphate (NADP+) that are essential for the generation of coenzymes[42]. Nicotinate treatment improved Glucose metabolism in KK-Ay obese mice[43] and nicotinamide prevented clinical disease in first-degree relatives of people with type-1 diabetes [44]. β-Nicotinamide mononucleotide is an important metabolite of the Nicotinate and nicotinamide metabolism pathway (Supplementary Fig. S9A). β-Nicotinamide mononucleotide is also a precursor of NAD+ and is considered a candidate compound for suppressing aging because it retained in the body for longer than Nicotinamide [45,46]. Thiamin is involved in several cell functions, including energy metabolism and the degradation of sugars and carbon skeletons [47]. Consuming too many simple carbohydrates automatically increases the need for Thiamin [48]. Thiamine pyrophosphate is the active form of thiamine and a member of the Thiamine metabolism pathway (Supplementary Fig. S9B)[49] deficiencies can lead to various forms of beriberi[50]. DL-Glutamine, also called L-Glutamine and Glutamine, is the most abundant amino acid in the body. Glutamine has many functions and is important in nutrition. A recent study has shown that adding enteral L-glutamine to normal nutrition during the early stage of COVID-19 infection can shorten the hospital stay for patients [51]. Hypoxanthine is an intermediate metabolite in the purine degradation system and a substrate for ATP synthesis. Hypoxanthine can reduce the severity of radiation damage by increasing the survival of endothelial cells from DNA damage and apoptosis in mice[52]. Traumatic acid, an oxidative derivative of unsaturated fatty acids, has anti-oxidative properties and can stimulate cell proliferation and protein kinase activity. Thus, Traumatic acid can be used to prevent and treat many blood circulation system diseases and skin diseases connected with oxidative stress[53]. Betaine is lipotropic, an important human nutrient, and dietary betaine was utilized as an osmolyte and source of methyl groups, thereby helping maintain liver, heart, and kidney health [54]. Uridine monophosphate, also called

5'-uridylic acid, is a ribonucleoside monophosphate. Dietary supplementation with uridine monophosphate can improve the growth performance of the piglets [55] and juvenile red sea bream [56] . Chaetocin is a natural metabolite isolated from Chaetomium fungi and can be used as a novel anticancer drug for its anticancer effect through inducing intrinsic and extrinsic apoptosis, cell cycle arrest, inhibition of migration and invasion, and suppression of cell proliferation [57].

5. Conclusion

Bmp6 is a key gene that regulates the development of intermuscular bones. In this study, we established a gene editing strategy for knocking out the two orthologs of *bmp6* in diploid crucian carp (*Carassius auratus*) more rapidly and obtained an F_3 population without IMBs (named WUCI strain). Extensive evaluation of the new strain's performance showed that the WUCI strain grew faster than the wild-type crucian carp at 4-month-age; The reproductive performance and flesh quality had no significant differences compared with wild-type crucian carp. In addition, the muscle tissues of the WUCI strain significantly enriched some metabolites plays beneficial effects in anti-aging, anti-oxidant, and anti-radiation damage. This is the first time to report a cyprinid strain without IMBs, which could be stably inherited, was obtained worldwide. This strain provides excellent germplasm for the cyprinids aquaculture industry and the two-round gene editing strategy is a useful molecular tool for eliminating IMBs in other cyprinids.

Conflict of Interest

The authors declare no competing financial interests.

Acknowledgments

We greatly thank Professor Ying Li at the Second Affiliated Hospital of Harbin Medical University for scanning mutants with X-ray and thank Dr. Yi Zhou at Harvard Medical School for providing technical support in CRISPR/Cas9. We also thank Professor Yumei Chang, Chitao Li, and Gefeng Xu at HRFRI for their support in the histological section and muscle texture analysis. This study was financially supported by the National Key R&D Program of China (no. 2018YFD0900102), Central Public-interest Scientific Institution Basal Research Fund, HRFRI (no. HSY202108Q, HYS201802Z), Central Public-interest Scientific Institution Basal Research Fund, CAFS (no. 2020XT0102).

Authors' contributions

Youyi Kuang and Xiaowen Sun conceived the study, Xianhu Zheng and Guangxiang Tong carried out the knockout of *bmp6*, Dingchen Cao and Zhipeng Sun cultured the fish, Huan Xu, Ting Yan, Tingting Zhang, Tan Zhang, Le Dong and Xiaoxing Yang carried out the mutant screening; Tingting Zhang, Tan Zhang, Huijie Zhou and Weilun Guo carried out the evaluation of the performance of WUCI strain, Shizhan Tang and Zhongxiang Chen carried out the determination of elements, Youyi Kuang and Huan Xu wrote the manuscript.

REFERENCES

[1] Sun Y, Zhu Z. Designing future farmed fishes using genome editing. Sci China Life Sci 2019;62:420–2. https://doi.org/10.1007/s11427-018-9467-x.

[2] Nie C, Hilsdorf AWS, Wan S, Gao Z. Understanding the development of intermuscular bones in teleost: status and future directions for aquaculture. Rev Aquacult 2020;12:759–72. https://doi.org/10.1111/raq.12348.

[3] Gui JF, Zhou L, Li XY. Rethinking fish biology and biotechnologies in the challenge era for burgeoning genome resources and strengthening food security. Water Biology Secur 2021;100002. https://doi.org/10.1016/j.watbs.2021.11.001.

[4] Meske C. Breeding carp for reduced number of intermuscular bones, and growth of carp in aquaria. Bamidgeh, Bulletin of Fish Culture in Israel 1968;20:105–19.

[5] Xu X, Zheng J, Qian Y, Luo C. Normally grown and developed intermuscular bone-deficient mutant in grass carp, Ctenopharyngodon idellus. Chinese Sci Bull 2015;60:52–7. https://doi.org/10.1360/n972014-00637.

[6] Perazza CA, Menezes JTB de, Ferraz JBS, Pinaffi FLV, Silva LA, Hilsdorf AWS. Lack of intermuscular bones in specimens of Colossoma macropomum: An unusual phenotype to be incorporated into genetic improvement programs. Aquaculture 2017;472:5760. https://doi.org/10.1016/j.aquaculture.2016.05.014.

[7] Wu C, Huang X, Chen Q, Hu F, Zhou L, Gong K, et al. The formation of a new type of hybrid culter derived from a hybrid lineage of Megalobrama amblycephala (♀) × Culter alburnus (♂). Aquaculture 2020;525:735328. https://doi.org/10.1016/j.aquaculture.2020.735328.

[8] Li L, Zhong Z, Zeng M, Liu S, Zhou Y, Xiao J, et al. Comparative analysis of intermuscular bones in fish of different ploidies. Sci China Life Sci 2013;56:341–50. https://doi.org/10.1007/s11427-013-4465-5.

[9] Cao DC., Kuang YY., Zheng XH., Tong GX., Li CT., Sun XW. Comparative analysis of intermuscular bones in three strains of common carp. J Appl Ichthyol 2015;31:32–6. https://doi.org/10.1111/jai.12483.

[10] Xiong XM, Robinson NA, Zhou JJ, Chen YL, Wang W, Wang XB, et al. Genetic parameter estimates for intermuscular bone in blunt snout bream (Megalobrama amblycephala) based on a microsatellite-based pedigree. Aquaculture 2019;502:371–7. https://doi.org/10.1016/j.aquaculture.2018.12.072.

[11] Wan S-M, Xiong XM, Tomljanović T, Chen YL, Liu H, Treer T, et al. Identification and mapping of SNPs associated with number of intermuscular bone in blunt snout bream. Aquaculture 2019;507:75–82. https://doi.org/10.1016/j.aquaculture.2019.04.013.

[12] Tang G, Lv W, Sun Z, Cao D, Zheng X, Tong G, et al. Heritability and quantitative trait locus analyses of intermuscular bones in mirror carp (Cyprinus carpio). Aquaculture 2020;515:734601. https://doi.org/10.1016/j.aquaculture.2019.734601.

[13] Nie C, Wan S, Chen Y, Zhu D, Wang X, Dong X, et al. Loss of scleraxis leads to distinct reduction of mineralized intermuscular bone in zebrafish. Aquac Fish 2021;6:169–77. https://doi.org/10.1016/j.aaf.2020.04.006.

[14] Kague E, Hughes SM, Lawrence EA, Cross S, Martin-Silverstone E, Hammond CL, et al. Scleraxis genes are required for normal musculoskeletal development and for rib growth and mineralization in zebrafish. Faseb J 2019;33:9116–30. https://doi.org/10.1096/fj.201802654rr.

[15] Xu H, Tong G, Yan T, Dong L, Yang X, Dou D, et al. Transcriptomic Analysis Provides Insights to Reveal the bmp6 Function Related to the Development of Intermuscular Bones in Zebrafish. Frontiers Cell Dev Biology 2022;10:821471. https://doi.org/10.3389/fcell.2022.821471.

[16] Yang J, Tong G, Sun Z, Zheng X, Lv W, Cao D, et al. Comparative Analysis of Muscle Development in Zebrafish with Different Intermuscular-Bones Patterns. Pak J Zool 2021;53:313–22. https://doi.org/10.17582/journal.pjz/20181125111102.

[17] Jian Y, Guangxiang T, Xianhu Z, Zhipeng S, Weihua L, Xiaowen S, et al. Comparative analysis of embryonic muscle development in wildtype zebrafish and its intermuscular bone deficiency mutant. Journal of Fishery Sciences of China 2019;26:296–303.https://doi.org/10.3724/SP.J.1118.2019.18119

[18] Yang J, Tong G, Zheng X, Sun Z, Lv W, Sun X, et al. Comparative analysis of skeletal development between wildtype zebrafish and intermuscular bone-deficient mutants. Acta Hydrobiologica Sinica 2020;44:546–53. https://doi.org/10.7541/2020.067

[19] Chen Z, Omori Y, Koren S, Shirokiya T, Kuroda T, Miyamoto A, et al. De novo assembly of the goldfish (Carassius auratus) genome and the evolution of genes after whole-genome duplication. Sci Adv 2019;5:eaav0547. https://doi.org/10.1126/sciadv.aav0547.

[20] Labun K, Montague TG, Krause M, Torres Cleuren YN, Tjeldnes H, Valen E. CHOPCHOP v3: expanding the CRISPR web toolbox beyond genome editing. Nucleic Acids Res 2019;47:W171–4. https://doi.org/10.1093/nar/gkz365.

[21] Tong G, Xu W, Zhang Y, Zhang Q, Yin J, Kuang Y. De novo assembly and characterization of the Hucho taimen transcriptome. Ecol Evol 2018;8:1271-1285. https://doi.org/10.1002/ece3.3735.

[22] Fiume M, Cupak M, Keenan S, Rambla J, Torre S de la, Dyke SOM, et al. CRISPResso2 provides accurate and rapid genome editing sequence analysis. Nat Biotechnol 2019;37:224–6. https://doi.org/10.1038/s41587-019-0032-3.

[23] Gan R-H, Wang Y, Li Z, Yu ZX, Li XY, Tong JF, et al. Functional Divergence of Multiple Duplicated Foxl2 Homeologs and Alleles in a Recurrent Polyploid Fish. Mol Biol Evol 2021;38:1995–2013. https://doi.org/10.1093/molbev/msab002.

[24] Franěk R, Kašpar V, Shah MA, Gela D, Pšenička M. Production of common carp donor-derived offspring from goldfish surrogate broodstock. Aquaculture 2021;534:736252. https://doi.org/10.1016/j.aquaculture.2020.736252.

[25] Kishi JY, Schaus TE, Gopalkrishnan N, Xuan F, Yin P. Programmable autonomous synthesis of single-stranded DNA. Nat Chem 2018;10:155–64. https://doi.org/10.1038/nchem.2872.

[26] Kishi JY, Lapan SW, Beliveau BJ, West ER, Zhu A, Sasaki HM, et al. SABER amplifies FISH: enhanced multiplexed imaging of RNA and DNA in cells and tissues. Nat Methods 2019;16:533–44. https://doi.org/10.1038/s41592-019-0404-0.

[27] Beliveau BJ, Kishi JY, Nir G, Sasaki HM, Saka SK, Nguyen SC, et al. OligoMiner provides a rapid, flexible environment for the design of genome-scale oligonucleotide in situ hybridization probes. Proc National Acad Sci 2018;115:201714530. https://doi.org/10.1073/pnas.1714530115.

[28] Pang Z, Zhou G, Ewald J, Chang L, Hacariz O, Basu N, et al. Using MetaboAnalyst 5.0 for LC–HRMS spectra processing, multi-omics integration and covariate adjustment of global metabolomics data. Nat Protoc 2022;17:1735–61. https://doi.org/10.1038/s41596-022-00710-w.

[29] Gjedrem T. Flesh quality improvement in fish through breeding. Aquaculture International 1997;5:197 206. https://doi.org/10.1023/a:1014546816984

[30] Wu RS, Lam II, Clay H, Duong DN, Deo RC, Coughlin SR. A Rapid Method for Directed Gene Knockout for Screening in G0 Zebrafish. Dev Cell 2018;46:112-125.e4. https://doi.org/10.1016/j.devcel.2018.06.003.

[31] Wan M, Cao X. BMP signaling in skeletal development. Biochem Bioph Res Co 2005;328:651–7. https://doi.org/10.1016/j.bbrc.2004.11.067.

[32] Jr B Andriopoulos, Corradini E, Xia Y, Faasse SA, Chen S, Grgurevic L, et al. BMP6 is a key endogenous regulator of hepcidin expression and iron metabolism. Nat Genet 2009;41:482–7. https://doi.org/10.1038/ng.335.

[33] Sugiura K, Su YQ, Eppig JJ. Does Bone Morphogenetic Protein 6 (BMP6) Affect Female Fertility in the Mouse?. Biol Reprod 2010;83:997–1004. https://doi.org/10.1095/biolreprod.110.086777.

[34] Campbell BK, Kendall NR, Baird DT. Effect of Direct Ovarian Infusion of Bone Morphogenetic Protein 6 (BMP6) on Ovarian Function in Sheep. Biol Reprod 2009;81:1016–23. https://doi.org/10.1095/biolreprod.109.076653.

[35] Solloway MJ, Dudley AT, Bikoff EK, Lyons KM, Hogan BLM, Robertson EJ. Mice lacking Bmp6 function. Dev Genet 1998;22:321–39. https://doi.org/10.1002/(sici)1520-6408(1998)22:4<321::aid-dvg3>3.0.co;2-8.

[36] Liu Y, Chen M, Zhao X, Ren X, Shao S, Zou M, et al. Bone morphogenetic protein 6 expression in cumulus cells is negatively associated with oocyte maturation. Hum Fertil 2019;24:290–7. https://doi.org/10.1080/14647273.2019.1660003.

[37] Song S, Ding W, Yao H, Wang L, Li B, Wang Y, et al. BMP6 Promotes the Secretion of 17 Beta-Estradiol and Progesterone in Goat Ovarian Granulosa Cells. Animals Open Access J Mdpi 2022;12:2132. https://doi.org/10.3390/ani12162132.

[38] Zhang X-Y, Chang HM, Zhu H, Liu RZ, Leung PCK. BMP6 increases TGF-β1 production by up-regulating furin expression in human granulosa-lutein cells. Cell Signal 2019;55:109–18. https://doi.org/10.1016/j.cellsig.2019.01.002.

[39] Lochab AK, Extavour CG. Bone Morphogenetic Protein (BMP) signaling in animal reproductive system development and function. Dev Biol 2017;427:258–69. https://doi.org/10.1016/j.ydbio.2017.03.002.

[40] Regan SLP, Knight PG, Yovich JL, Leung Y, Arfuso F, Dharmarajan A. Chapter Nine Involvement of Bone Morphogenetic Proteins (BMP) in the Regulation of Ovarian Function. Vitam Horm 2018;107:227–61. https://doi.org/10.1016/bs.vh.2018.01.015.

[41] Li CW, Ge W. Spatiotemporal Expression of Bone Morphogenetic Protein Family Ligands and Receptors in the Zebrafish Ovary: A Potential Paracrine-Signaling Mechanism for Oocyte-Follicle Cell Communication. Biol Reprod 2011;85:977–86. https://doi.org/10.1095/biolreprod.111.092239.

[42] Information N Center for Biotechnology. PubChem Pathway Summary for Pathway SMP0087241, Nicotinate and Nicotinamide Metabolism, Source: PathBank. Retrieved November 15, 2022 from https://pubchem.ncbi.nlm.nih.gov/pathway/PathBank:SMP0087241.

[43] Yoshinari O, Igarashi K. Anti-diabetic effect of trigonelline and nicotinic acid, on KK-A(y) mice. Curr Med Chem 2010;17:2196–202. https://doi.org/10.2174/092986710791299902.

[44] Olmos PR, Hodgson MI, Maiz A, Manrique M, Valdés MDD, Foncea R, et al. Nicotinamide protected first-phase insulin response (FPIR) and prevented clinical disease in first-degree relatives of type-1 diabetics. Diabetes Res Clin Pr 2006;71:320–33. https://doi.org/10.1016/j.diabres.2005.07.009.

[45] Kawamura T, Mori N, Shibata K. β-Nicotinamide Mononucleotide, an Anti-Aging Candidate Compound, Is Retained in the Body for Longer than Nicotinamide in Rats. J Nutr Sci Vitaminol 2016;62:272–6. https://doi.org/10.3177/jnsv.62.272.

[46] Nadeeshani H, Li J, Ying T, Zhang B, Lu J. Nicotinamide Mononucleotide (NMN) as an Anti-Aging Health Product - Promises and Safety Concerns. J Adv Res 2021;37:267–78. https://doi.org/10.1016/j.jare.2021.08.003.

[47] Manzetti S, Zhang J, Spoel D van der. Thiamin Function, Metabolism, Uptake, and Transport. Biochemistry 2014;53:821–35. https://doi.org/10.1021/bi401618y.

[48] Derrick L. A Review of the Biochemistry, Metabolism and Clinical Benefits of Thiamin(e) and Its Derivatives. Evid-Based Compl Alt 2006;3:49–59. https://doi.org/10.1093/ecam/nek009.

[49] Zeece M. Introduction to the Chemistry of Food 2020:163–212. https://doi.org/10.1016/b978-0-12-809434-1.00005-0.

[50] Nohr D, Biesalski HK, Back EI. Encyclopedia of Dairy Sciences (Second Edition). Article Titles V 2011:701–3. https://doi.org/10.1016/b978-0-12-374407-4.00490-8.

[51] Cengiz M, Uysal BB, Ikitimur H, Ozcan E, Islamoğlu MS, Aktepe E, et al. Effect of oral l-Glutamine supplementation on Covid-19 treatment. Clin Nutrition Exp 2020;33:24–31. https://doi.org/10.1016/j.yclnex.2020.07.003.

[52] Fujiwara M, Sato N, Okamoto K. Hypoxanthine Reduces Radiation Damage in Vascular Endothelial Cells and Mouse Skin by Enhancing ATP Production via the Salvage Pathway. Radiat Res 2022;197:583–93. https://doi.org/10.1667/rade-21-00223.1.

[53] Jabłońska-Trypuć A, Pankiewicz W, Czerpak R. Traumatic Acid Reduces Oxidative Stress and Enhances Collagen Biosynthesis in Cultured Human Skin Fibroblasts. Lipids 2016;51:1021–35. https://doi.org/10.1007/s11745-016-4174-5.

[54] Craig SA. Betaine in human nutrition. Am J Clin Nutrition 2004;80:539–49. https://doi.org/10.1093/ajcn/80.3.539.

[55] Li B, Zhou H, Wu X, Chen Z, Yao J, Yin Y. Effects of dietary supplementation with uridine monophosphate on performance and intestinal morphology of weanling piglets. J Anim Sci 2016;94:82–6. https://doi.org/10.2527/jas.2015-9440.

[56] Hossain MdS, Koshio S, Ishikawa M, Yokoyama S, Sony NM. Dietary supplementation of uridine monophosphate enhances growth, hematological profile, immune functions and stress tolerance of juvenile red sea bream, Pagrus major. Aquaculture 2017;475:29–39. https://doi.org/10.1016/j.aquaculture.2017.04.008.

[57] Jiang H, Li Y, Xiang X, Tang Z, Liu K, Su Q, et al. Chaetocin: A review of its anticancer potentials and mechanisms. Eur J Pharmacol 2021;910:174459. https://doi.org/10.1016/j.ejphar.2021.174459.

Figure legends

Fig. 1. Expression of *bmp6a* and *bmp6b* in tissues of crucian carp. (a) the gene tree of *bmp6a* and *bmp6b*, the tree was extracted from Ensembl. (b) the expression of *bmp6a* and *bmp6b* in crucian carp tissues analyzed by qPCR, electrophoretic images were cropped from the original images in Supplementary Figs. S1, S2. M: molecular marker. (c) the relative expression levels of *bmp6a* and *bmp6b* in crucian carp tissues analyzed by real-time quantitative PCR. (d) and (e) spatial expression of *bmp6a* (d) and *bmp6b* (e) in caudal muscle, the white dashed lines indicate myospetum; scale bar: 100μm.

Fig. 2. Pipeline for generating the new crucian carp strain without intermuscular bones. (a) the schematic diagram for constructing the new strain without intermuscular bones. (b) target sites of *bmp6a* and *bmp6b* for CRISPR/Cas9 knockout. (c) the schematic diagram for screening mutants. (d) the somatic mutation distribution of mutants in the F_0 and F_1 generation. E, the somatic mutation distribution of mutants with both genes mutated in the F_0 and F_1 generation.

Fig. 3. Observation of intermuscular bones in mutants of F_1, F_2, and F_3 generations. (a) micro-CT images of a wild-type crucian carp(top) and a representative mutant without intermuscular bones in the F_1 generation(bottom). (b) X-ray images of a wild-type crucian carp (top left) and representative mutants of *bmp6a*$^{-/-}$ (top right), *bmp6b*$^{-/-}$ mutant (bottom left), and *bmp6a*$^{-/-}$/*bmp6b*$^{-/-}$ (bottom right) in the F_2 generation. (c) X-ray images of a wild-type crucian carp(top) and a representative mutant without intermuscular bones(bottom) in the F_3 generation. (d) skeletal staining images of a wild-type crucian carp(top) and a representative mutant

without intermuscular bones(bottom) in the F_3 generation, 41 individuals were randomly chosen for bone staining, and no intermuscular bones were observed; top left, caudal skeleton; top right, dorsal skeleton. The scale bar in B and C was 10mm, and the scale bar in D was 2000μm.

Fig. 4. Growth performance of the new strain without intermuscular bones and the wild-type crucian carp. The body length (SL, a) and body weight (BW, d) were measured at the age of 2, 3, and 4 months, the increment of SL(b) and BW(e) per month and the specific growth rate per month of SL(c) and BW(f) was calculated. The summary of BW and SL were listed in Supplementary Table S7. The significant difference was tested using Student's t-test. WT: the wild-type crucian carp; WUCI: the new strain without intermuscular bones; *: $P<0.05$; **: $P<0.01$; ***: $P<0.001$; ****: $P<0.0001$; ns: no significance.

Fig. 5. Nutrient quality of the new strain without intermuscular bones and the wild-type crucian carp. Proximate composition(a), total saccharide(b), vitamins(c), amino acid composition(d), and fatty acid (e, f) were determined. The data used to draw these figures were shown in Supplementary Table S8-S11. Wilcox test was used to test the significant levels (n=3). WT: the wild-type crucian carp; WUCI: the new strain without intermuscular bones; Ash: crude ash; Fat: crude fat; Protein: crude protein; Saccharide: total saccharide; VB1: vitamin B1; VB2: vitamin B2; VE: vitamin E; EAA: essential amino acid; TAA: total amino acid; UAA: umami amino acid; EFA: essential fatty acid; Saturated: saturated fatty acid; TFA: total fatty acid; Unsaturated: unsaturated fatty acid; MUFA: monounsaturated fatty acid; PUFA: polyunsaturated fatty acid; Omega3: omega3 fatty acid; Omega6: omega6 fatty acid; ns: no significance.

Fig. 6. Content of 7 elements in the new strain without intermuscular bones and the wild-type crucian carp. The contents of Mg(a), Mn(b), Fe(c), Cu(d), Zn(e), Se(f), and K(g) in the new strain, and the wild-type crucian carp were determined using the dorsal muscle and liver tissues. The data used to draw these figures were listed in Supplementary Table S12. Wilcox test was used to test the significant levels(n=5). WT: the wild-type crucian carp; WUCI: the new strain without intermuscular bones; *: $P<0.05$; ns: no significance.

Fig. 7. Muscle texture and structure of the new strain without intermuscular bones and the wild-type crucian carp. The shear force(a), hardness(b), cohesiveness(c), springiness(d), gumminess(e), and chewiness(f) were tested using a texture meter; Student' s t-test was used to test the significant levels(n=30). The histological sections were carried out using dorsal muscle in the wild-type crucian carp(i) and the new strain(j), and the area(g) and density(h) of muscle fibers were calculated using the histological images with the ImageJ program, Wilcox test(n=5) was used to test the significant levels. The data used to draw the figures were shown in Supplementary Table S13. The scale bar in (i) and (j) was 50μm. WT: the wild-type crucian carp; WUCI: the new strain without intermuscular bones; *: $P<0.05$; **: $P<0.01$; ns: no significance.

Fig. 8. Reproductive performance of the new strain and the wild-type crucian carp. The weight of gonad(a), gonad index (GSI, b), female absolute fecundity(c), and relative fecundity(d) were compared between the 4-months-old individuals of the

new strain and the wild-type crucian carp. The data used to draw the figures were shown in Supplementary Table S14; the Wilcox test was used to test the significant levels. E, histological sections of gonads in the wild-type crucian carp and the new strain, the scale bar in ovary and testis tissues was 100μm and 20μm, respectively. WT: the wild-type crucian carp; WUCI: the new strain without intermuscular bones; I(black arrowhead), II, III, and IV represent the developmental phases of oocytes; sg: Spermatogonium; sc: spermatocytes; SZ: Spermatozoa; *: $P<0.05$; ns: no significance.

Fig. 9. Metabolomics analysis of the new strain and the wild-type crucian carp. (a, b) the PCA analysis of the metabolites in positive ion mode(a) and negative ion mode(b); (c, d) the PLS-DA analysis of the metabolites in positive ion mode(c) and negative ion mode(d); (e) the enriched pathways of metabolites in muscle tissue of the new strain analyzed by MetaboAnalyst 5.0. WT_M: muscle of wild-type crucian; WUCI_M: muscle of the new strain without intermuscular bones.

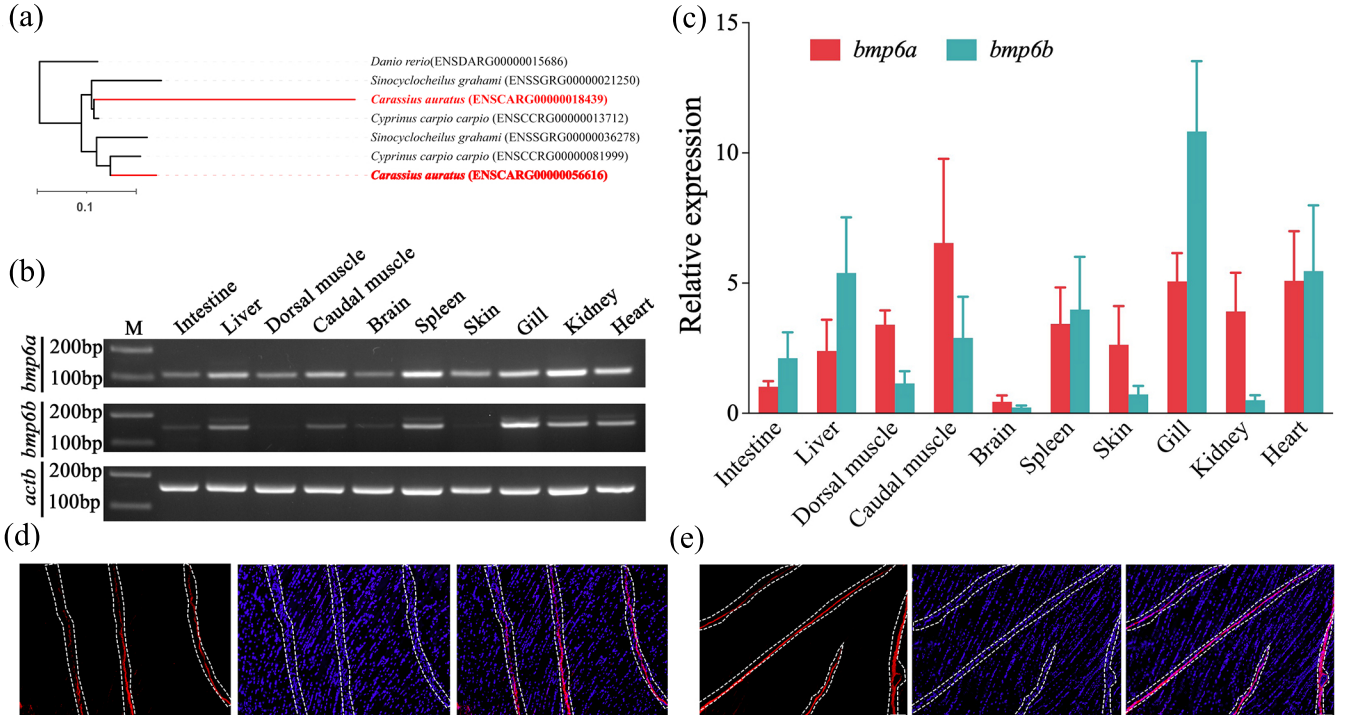
(a)
Danio rerio(ENSDARG00000015686)
Sinocyclocheilus grahami (ENSSGRG00000021250)
Carassius auratus (ENSCARG00000018439)
Cyprinus carpio carpio (ENSCCRG00000013712)
Sinocyclocheilus grahami (ENSSGRG00000036278)
Cyprinus carpio carpio (ENSCCRG00000081999)
Carassius auratus (ENSCARG00000056616)
0.1
(b)
M
Intestine
Liver
Dorsal muscle
Caudal muscle
Brain
Spleen
Skin
Gill
Kidney
Heart
bmp6a
bmp6b
actb
200bp
100bp
(c)
bmp6a
bmp6b
Relative expression
0
5
10
15
Intestine
Liver
Dorsal muscle
Caudal muscle
Brain
Spleen
Skin
Gill
Kidney
Heart
(d)
(e)

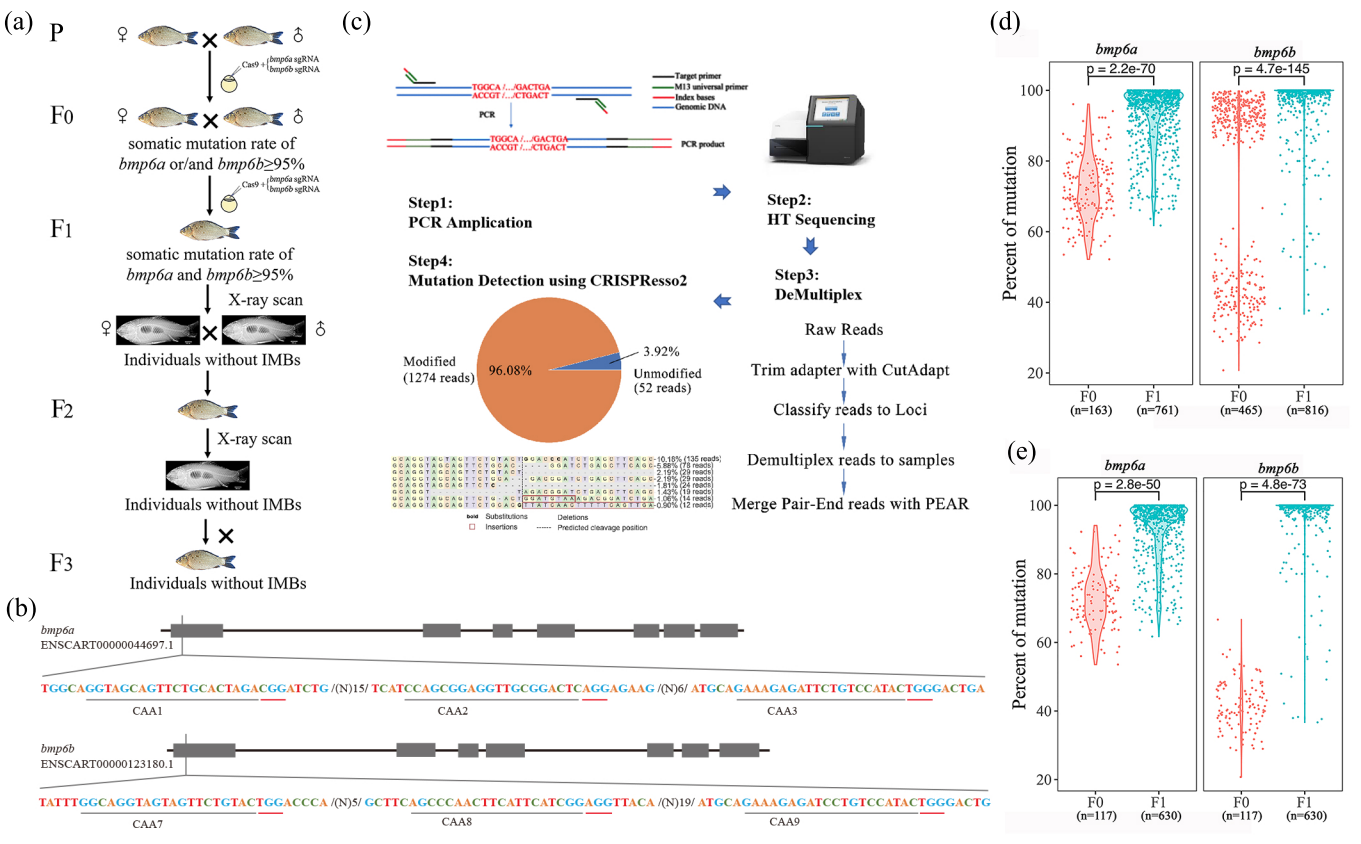
(a)
P
Cas9 + bmp6a sgRNA bmp6b sgRNA
F0
somatic mutation rate of bmp6a or/and bmp6b≥95%
Cas9 + bmp6a sgRNA bmp6b sgRNA
F1
somatic mutation rate of bmp6a and bmp6b≥95%
X-ray scan
Individuals without IMBs
F2
X-ray scan
Individuals without IMBs
F3
Individuals without IMBs
(c)
TGGCA /.../GACTGA
ACCGT /.../CTGACT
PCR
TGGCA /.../GACTGA
ACCGT /.../CTGACT
PCR product
Target primer
M13 universal primer
Index bases
Genomic DNA
Step1:
PCR Amplication
Step2:
HT Sequencing
Step3:
DeMultiplex
Step4:
Mutation Detection using CRISPResso2
Modified
(1274 reads)
96.08%
3.92%
Unmodified
(52 reads)
10.18% (135 reads)
5.88% (78 reads)
2.19% (29 reads)
2.19% (29 reads)
1.81% (24 reads)
1.43% (19 reads)
1.06% (14 reads)
0.90% (12 reads)
base Substitutions
Insertions
Deletions
Predicted cleavage position
Raw Reads
Trim adapter with CutAdapt
Classify reads to Loci
Demultiplex reads to samples
Merge Pair-End reads with PEAR
(b)
bmp6a
ENSCART00000044697.1
TGGCAGGTAGCAGTTCTGCACTAGACGGATCTG /(N)15/ TCATCCAGCGGAGGTTGCGGACTCAGGAGAAG /(N)6/ ATGCAGAAAGAGATTCTGTCCATACTGGGACTGA
CAA1
CAA2
CAA3
bmp6b
ENSCART00000123180.1
TATTTGGCAGGTAGTAGTTCTGTACTGGACCCA /(N)5/ GCTTCAGCCCAACTTCATTCATCGGAGGTTACA /(N)19/ ATGCAGAAAGAGATCCTGTCCATACTGGGACTG
CAA7
CAA8
CAA9
(d)
bmp6a
bmp6b
p = 2.2e-70
p = 4.7e-145
Percent of mutation
F0 (n=163)
F1 (n=761)
F0 (n=465)
F1 (n=816)
(e)
bmp6a
bmp6b
p = 2.8e-50
p = 4.8e-73
Percent of mutation
F0 (n=117)
F1 (n=630)
F0 (n=117)
F1 (n=630)

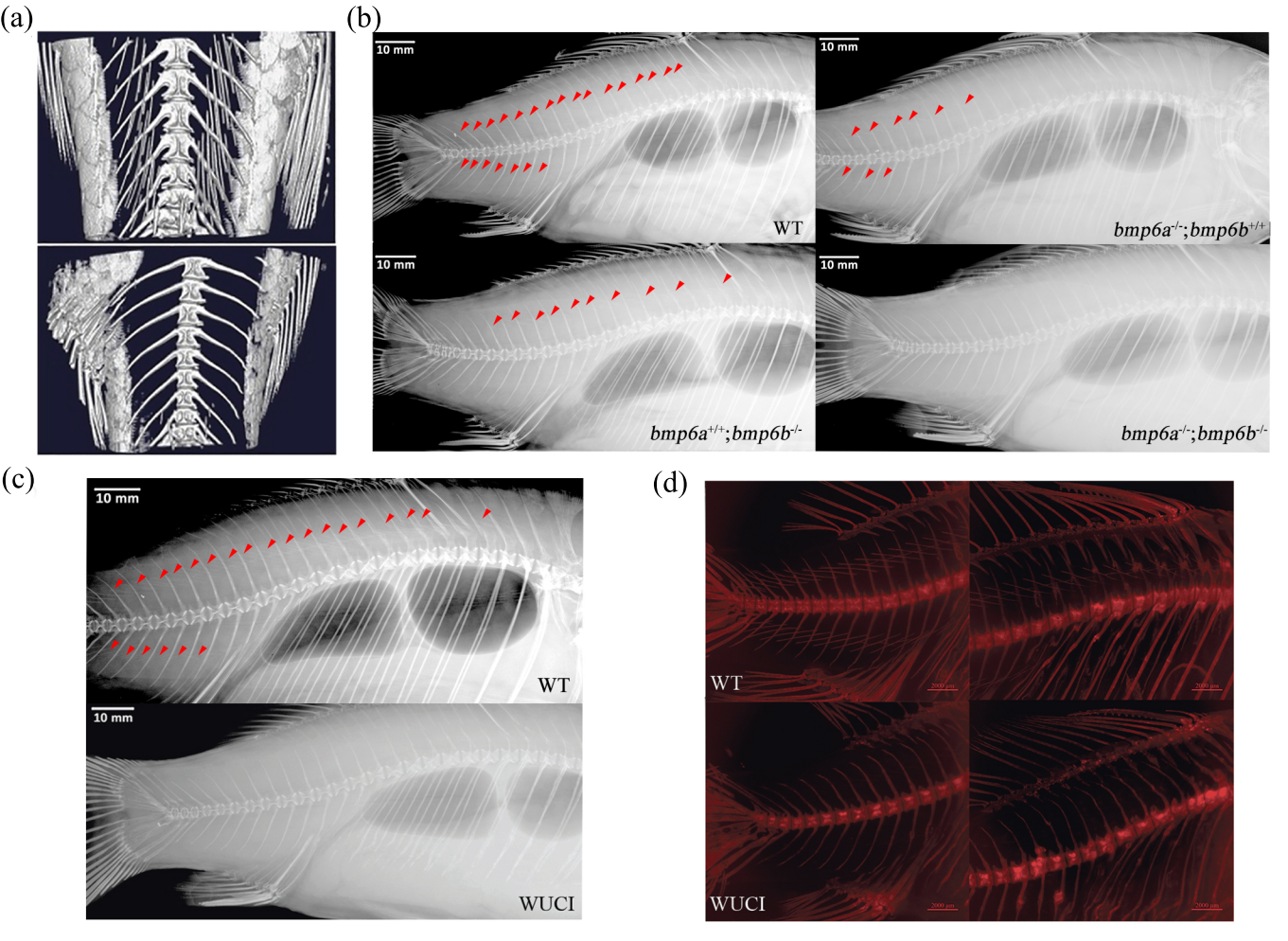
(a)
(b)
10 mm
WT
10 mm
bmp6a-/-;bmp6b+/+
10 mm
bmp6a+/+;bmp6b-/-
10 mm
bmp6a-/-;bmp6b-/-
(c)
10 mm
WT
10 mm
WUCI
(d)
WT
WUCI

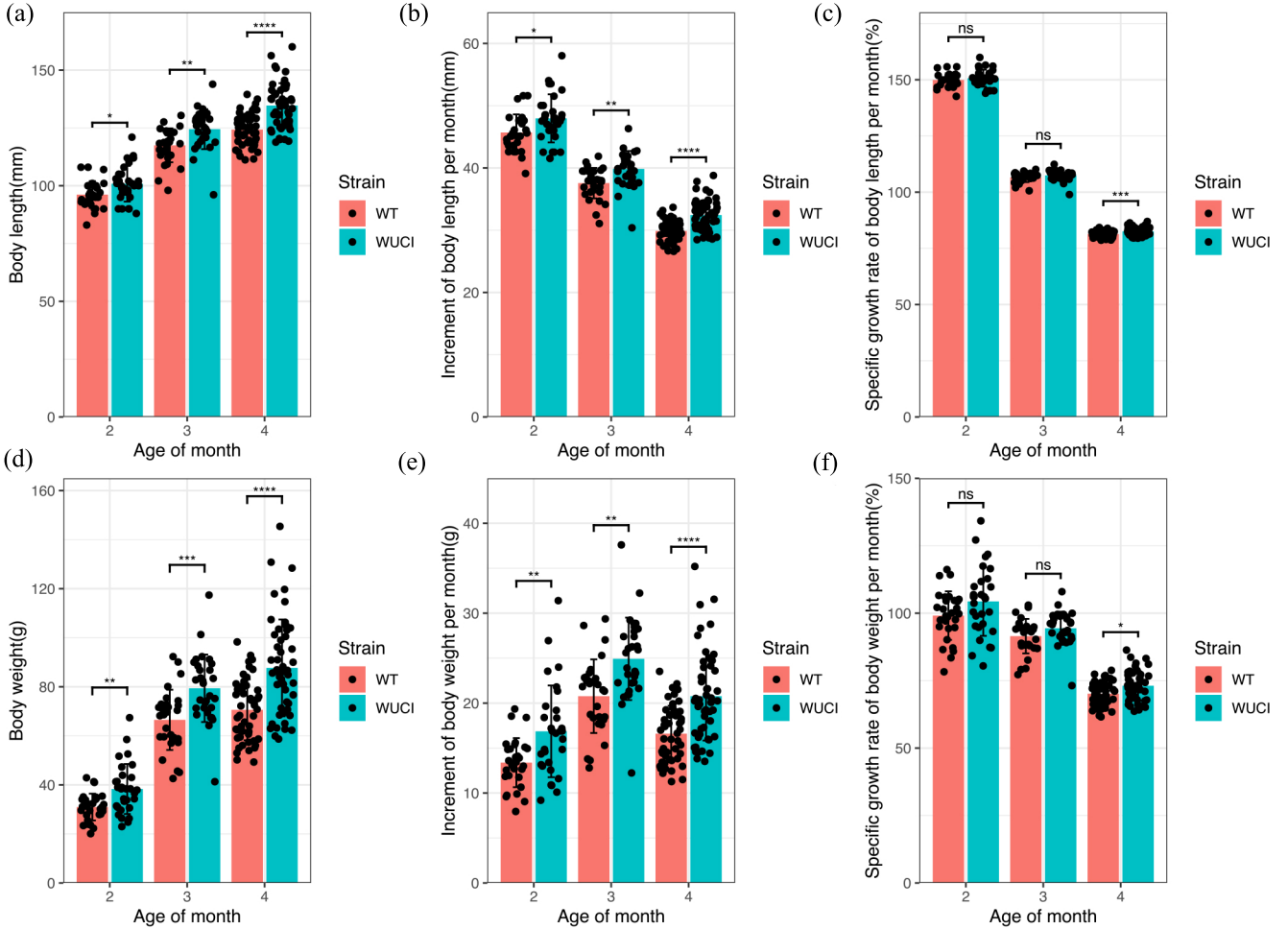
(a)
Body length(mm)
Age of month
Strain
WT
WUCI
(b)
Increment of body length per month(mm)
Age of month
Strain
WT
WUCI
(c)
Specific growth rate of body length per month(%)
Age of month
Strain
WT
WUCI
(d)
Body weight(g)
Age of month
Strain
WT
WUCI
(e)
Increment of body weight per month(g)
Age of month
Strain
WT
WUCI
(f)
Specific growth rate of body weight per month(%)
Age of month
Strain
WT
WUCI

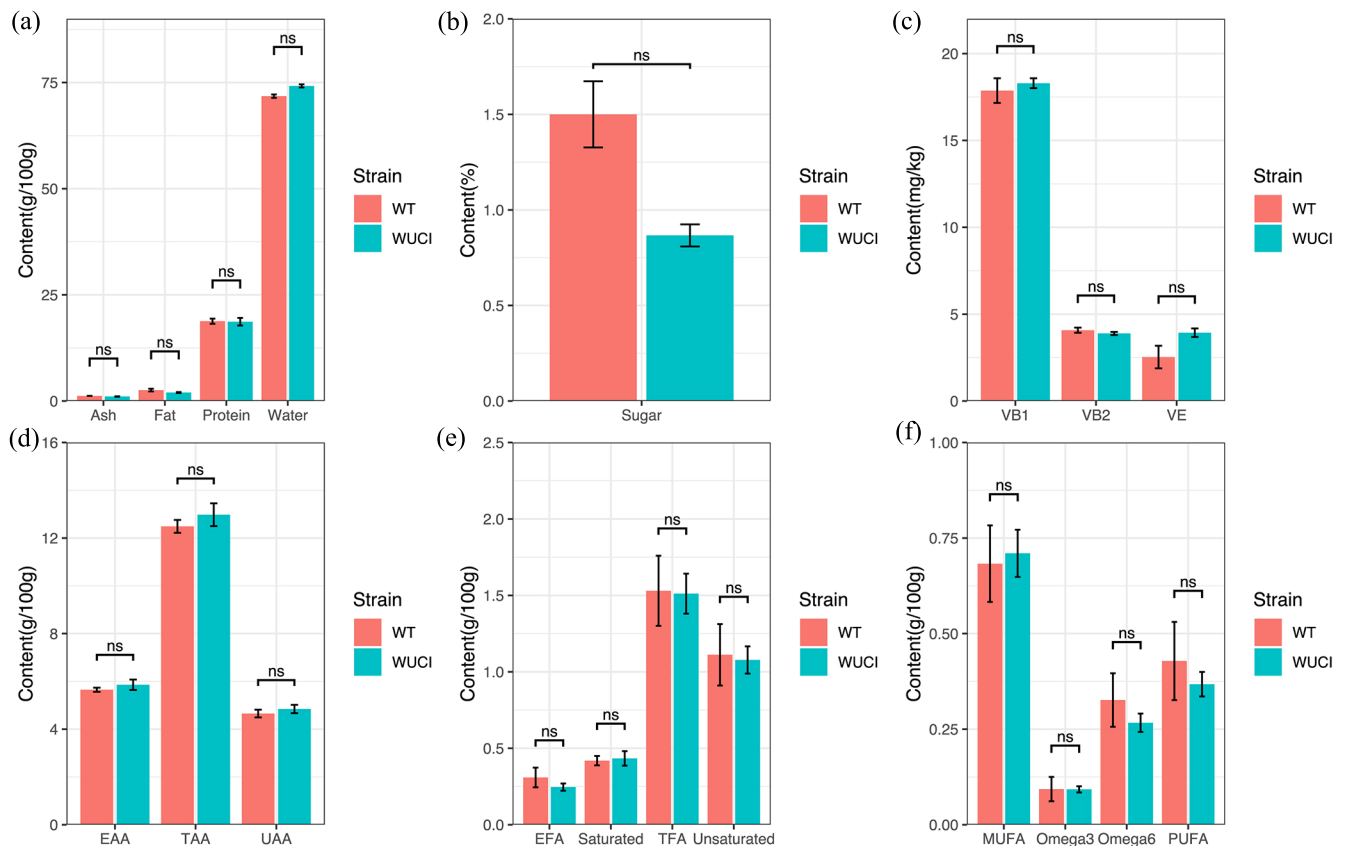
(a)
Content(g/100g)
ns
Ash
Fat
Protein
Water
Strain
WT
WUCI
(b)
Content(%)
Sugar
(c)
Content(mg/kg)
VB1
VB2
VE
(d)
EAA
TAA
UAA
(e)
EFA
Saturated
TFA
Unsaturated
(f)
MUFA
Omega3
Omega6
PUFA

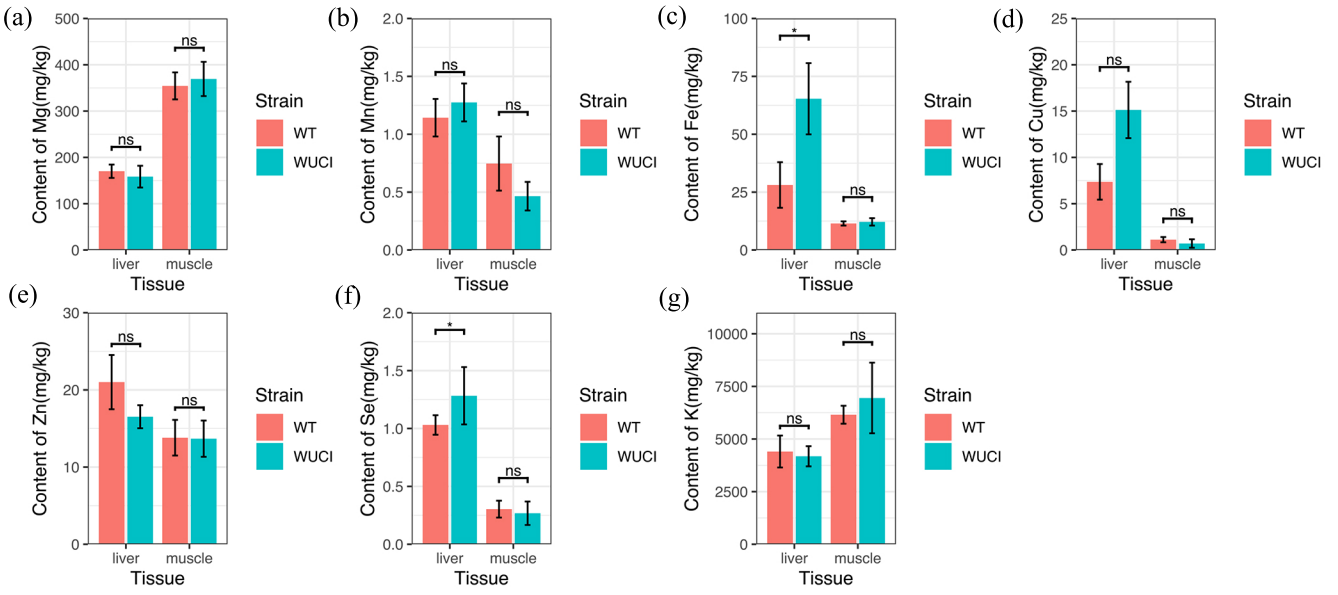
(a)
Content of Mg(mg/kg)
500
400
300
200
100
0
ns
ns
liver
muscle
Tissue
Strain
WT
WUCI
(b)
Content of Mn(mg/kg)
2.0
1.5
1.0
0.5
0.0
ns
ns
liver
muscle
Tissue
Strain
WT
WUCI
(c)
Content of Fe(mg/kg)
100
75
50
25
0
*
ns
liver
muscle
Tissue
Strain
WT
WUCI
(d)
Content of Cu(mg/kg)
25
20
15
10
5
0
ns
ns
liver
muscle
Tissue
Strain
WT
WUCI
(e)
Content of Zn(mg/kg)
30
20
10
0
ns
ns
liver
muscle
Tissue
Strain
WT
WUCI
(f)
Content of Se(mg/kg)
2.0
1.5
1.0
0.5
0.0
*
ns
liver
muscle
Tissue
Strain
WT
WUCI
(g)
Content of K(mg/kg)
10000
7500
5000
2500
0
ns
ns
liver
muscle
Tissue
Strain
WT
WUCI

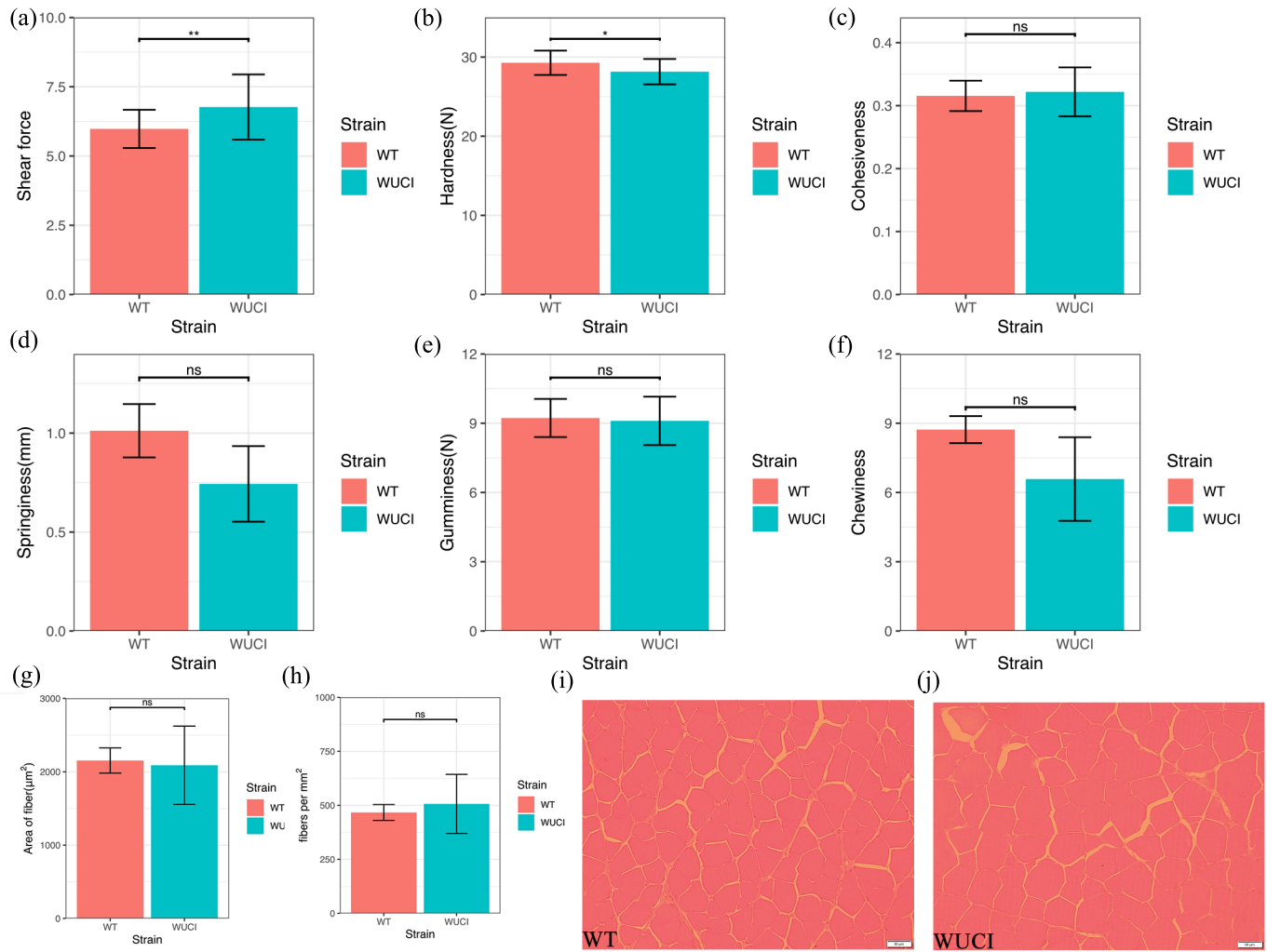
(a)
Shear force
10.0
7.5
5.0
2.5
0.0
**
WT
WUCI
Strain
Strain
WT
WUCI
(b)
Hardness(N)
30
20
10
0
*
WT
WUCI
Strain
Strain
WT
WUCI
(c)
Cohesiveness
0.4
0.3
0.2
0.1
0.0
ns
WT
WUCI
Strain
Strain
WT
WUCI
(d)
Springiness(mm)
1.0
0.5
0.0
ns
WT
WUCI
Strain
Strain
WT
WUCI
(e)
Gumminess(N)
12
9
6
3
0
ns
WT
WUCI
Strain
Strain
WT
WUCI
(f)
Chewiness
12
9
6
3
0
ns
WT
WUCI
Strain
Strain
WT
WUCI
(g)
Area of fiber(μm²)
3000
2000
1000
0
ns
WT
WUCI
Strain
Strain
WT
WU
(h)
fibers per mm²
1000
750
500
250
0
ns
WT
WUCI
Strain
Strain
WT
WUCI
(i)
WT
(j)
WUCI

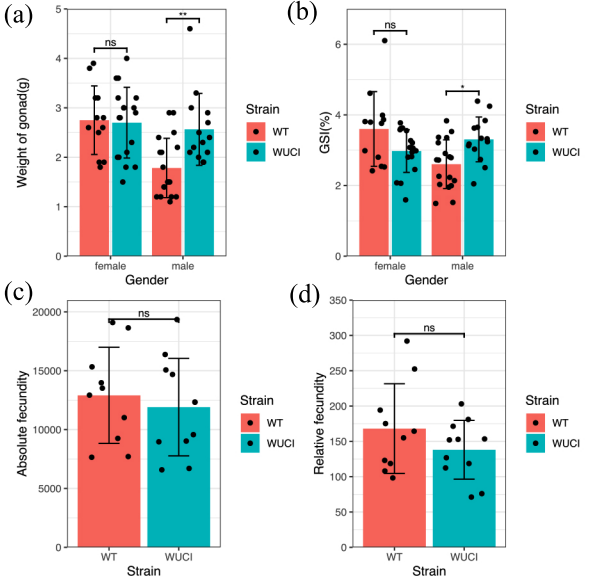
(a)
Weight of gonad(g)
ns
**
female
male
Gender
Strain
WT
WUCI
(b)
GSI(%)
ns
*
female
male
Gender
Strain
WT
WUCI
(c)
Absolute fecundity
ns
WT
WUCI
Strain
Strain
WT
WUCI
(d)
Relative fecundity
ns
WT
WUCI
Strain
Strain
WT
WUCI

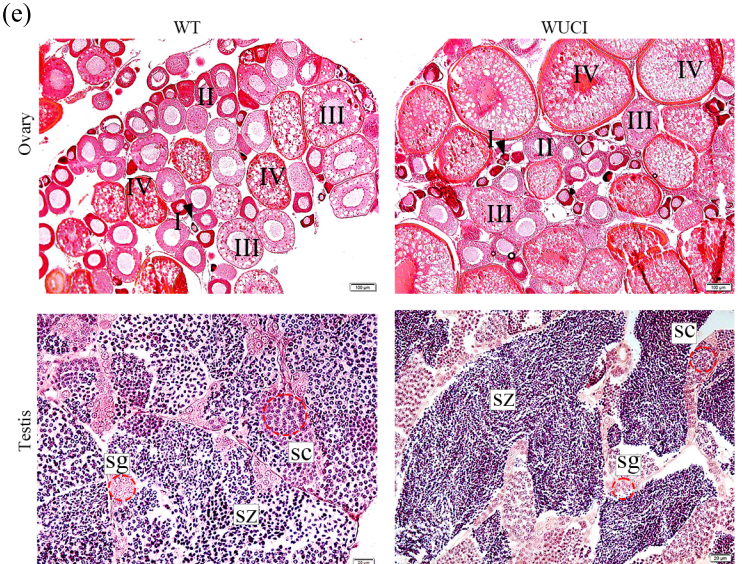
(e)
WT
WUCI
Ovary
Testis
I
II
III
IV
sg
sc
SZ

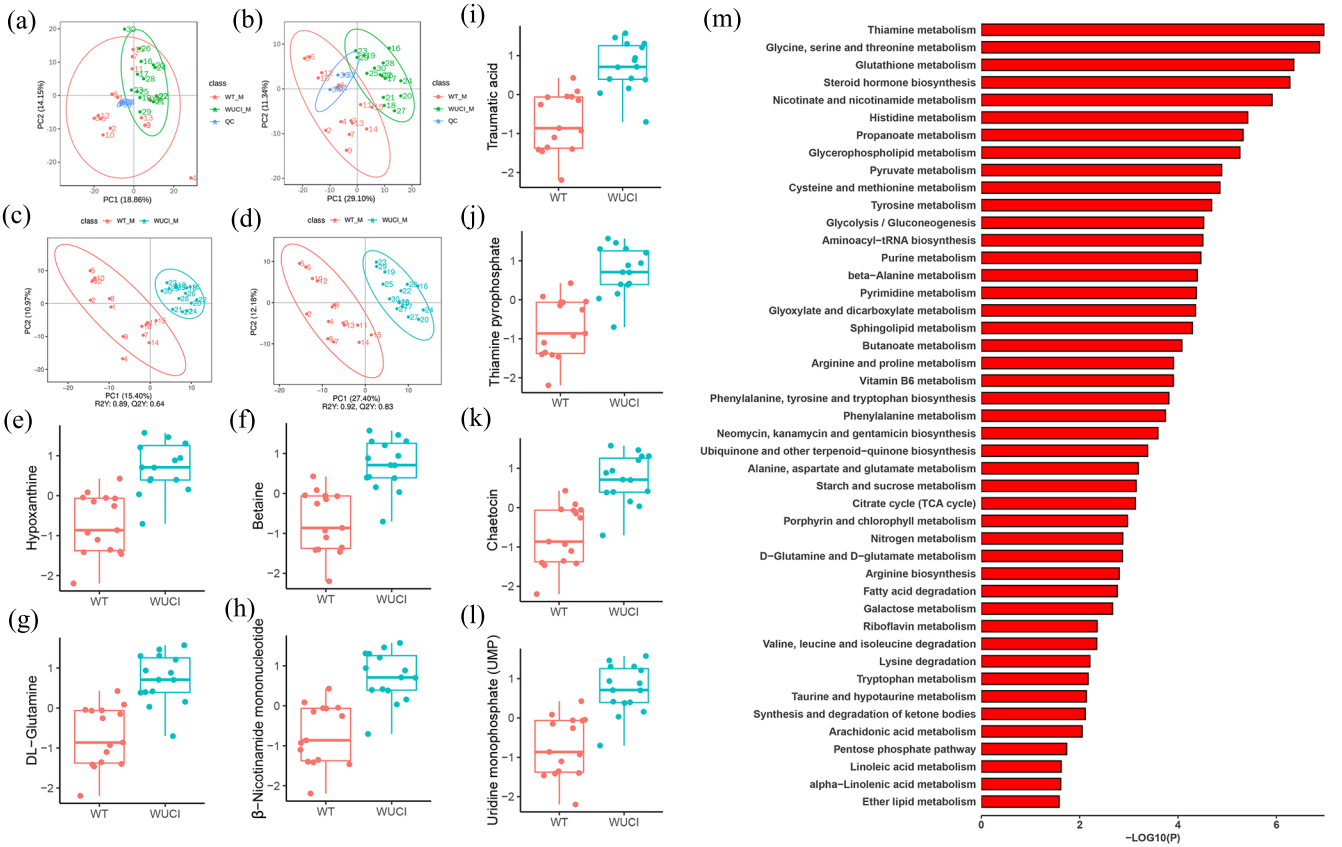
(a)
PC1 (18.86%)
PC2 (14.15%)
class
WT_M
WUCI_M
QC
(b)
PC1 (29.10%)
PC2 (11.34%)
(c)
PC1 (15.40%)
PC2 (10.97%)
R2Y: 0.89, Q2Y: 0.64
(d)
PC1 (27.40%)
PC2 (12.18%)
R2Y: 0.92, Q2Y: 0.83
(e)
Hypoxanthine
(f)
Betaine
(g)
DL−Glutamine
(h)
β−Nicotinamide mononucleotide
(i)
Traumatic acid
(j)
Thiamine pyrophosphate
(k)
Chaetocin
(l)
Uridine monophosphate (UMP)
WT
WUCI
(m)
Thiamine metabolism
Glycine, serine and threonine metabolism
Glutathione metabolism
Steroid hormone biosynthesis
Nicotinate and nicotinamide metabolism
Histidine metabolism
Propanoate metabolism
Glycerophospholipid metabolism
Pyruvate metabolism
Cysteine and methionine metabolism
Tyrosine metabolism
Glycolysis / Gluconeogenesis
Aminoacyl−tRNA biosynthesis
Purine metabolism
beta−Alanine metabolism
Pyrimidine metabolism
Glyoxylate and dicarboxylate metabolism
Sphingolipid metabolism
Butanoate metabolism
Arginine and proline metabolism
Vitamin B6 metabolism
Phenylalanine, tyrosine and tryptophan biosynthesis
Phenylalanine metabolism
Neomycin, kanamycin and gentamicin biosynthesis
Ubiquinone and other terpenoid−quinone biosynthesis
Alanine, aspartate and glutamate metabolism
Starch and sucrose metabolism
Citrate cycle (TCA cycle)
Porphyrin and chlorophyll metabolism
Nitrogen metabolism
D−Glutamine and D−glutamate metabolism
Arginine biosynthesis
Fatty acid degradation
Galactose metabolism
Riboflavin metabolism
Valine, leucine and isoleucine degradation
Lysine degradation
Tryptophan metabolism
Taurine and hypotaurine metabolism
Synthesis and degradation of ketone bodies
Arachidonic acid metabolism
Pentose phosphate pathway
Linoleic acid metabolism
alpha−Linolenic acid metabolism
Ether lipid metabolism
−LOG10(P)